Eur. Phys. J. E **15**, 319–333 (2004)
DOI 10.1140/epje/i2004-10074-4

THE EUROPEAN PHYSICAL JOURNAL E

Nonequilibrium fluctuations in the Rayleigh-Bénard problem for binary fluid mixtures

J.M. Ortiz de Zárate[1,a], F. Peluso[2], and J.V. Sengers[3]

[1] Departamento de Física Aplicada 1, Facultad de Ciencias Físicas, Universidad Complutense, E-28040 Madrid, Spain
[2] Microgravity Advanced Research and user Support (MARS) Center srl, via Emanuele Gianturco 31, I-80146 Napoli, Italy
[3] Institute for Physical Science and Technology and Departments of Chemical and Mechanical Engineering, University of Maryland, College Park, MD 20742, USA

Received 22 July 2004 and Received in final form 10 October 2004 /
Published online: 18 November 2004 –

Abstract. We have employed a simple Galerkin-approximation scheme to calculate nonequilibrium temperature and concentration fluctuations in a binary fluid subjected to a temperature gradient with realistic boundary conditions. When a fluid mixture is driven outside thermal equilibrium, there are two instability mechanisms, namely a Rayleigh (stationary) and a Hopf (oscillatory) instability, causing long-ranged fluctuations. The competition of these two mechanisms causes the structure factor associated with the temperature fluctuations to exhibit two maxima as a function of the wave number q of the fluctuations, in particular, close to the convective instability. In the presence of thermally conducting but impermeable walls the intensity of the temperature fluctuations vanishes as q goes to zero, while the intensity of the concentration fluctuations remains finite in the limit of vanishing q. Finally, we propose a simpler small-Lewis-number approximation scheme, which is useful to represent nonequilibrium concentration fluctuations for mixtures with positive separation ratio, even close to (but below) the convective instability.

PACS. 05.40.-a Fluctuation phenomena, random processes, noise, and Brownian motion – 47.20.Bp Buoyancy-driven instability – 47.54.+r Pattern selection; pattern formation – 78.35.+c Brillouin and Rayleigh scattering; other light scattering

1 Introduction

This paper is concerned with the enhancement of fluctuations in a binary liquid mixture that is outside equilibrium because of the presence of a (moderate) temperature gradient, but that is still in a quiescent conductive state below the convective instability. In principle, the wave number dependence of the nonequilibrium structure factor can be determined experimentally with light scattering or shadowgraph techniques [1]. The shadowgraph technique has the advantage, compared to light scattering, of being able to access the very small wave numbers needed to study fluctuations close to convective instabilities. However, to visualize the thermal fluctuations with the shadowgraph method, one needs to perform the experiments with a fluid in which the thermal noise is already large in equilibrium. For one-component fluids, this goal has been accomplished by performing shadowgraph experiments in a supercritical fluid not far from its critical point [2]. However, for a fluid in the critical region, a detailed interpretation of the experiments is complicated by the presence of non-Boussinesq effects. This problem can be avoided for binary fluids, where the thermal nonequilibrium fluctuations are dominated by strong Soret-driven concentration fluctuations [3,4], so that shadowgraph experiments can be performed in fluid mixtures far away from any critical point [5], where a simple Boussinesq approximation is adequate.

For the interpretation of such experiments, a theoretical investigation of nonequilibrium fluctuations in a binary mixture is required. Hence, we have extended our previous work for one-component fluids [6], and developed a quantitative theory for the nonequilibrium structure factor of binary fluid mixtures below the onset of Rayleigh-Bénard convection using linearized fluctuating hydrodynamics in the Boussinesq approximation. As some previous investigators [7], we take into account buoyancy, but the main innovation of the present paper is that we also consider boundary conditions, which are expected to become important when the wavelength of the fluctuations becomes of the order of the size of the system. In a previous publication [8], we considered the unrealistic case of two free and permeable walls. In the present paper, we consider more realistic boundary conditions. To incorporate such

[a] e-mail: jmortizz@fis.ucm.es

realistic boundary conditions in the derivation of the nonequilibrium structure factor, we shall use a Galerkin approximation, as was done previously for the case of a one-component fluid [6]. Specifically, we adopt the same set of Galerkin test functions previously used by Lhost *et al.* [9] to describe the convection threshold in binary mixtures, for both positive and negative separation ratios.

First, we shall recover the well-known [10] q^{-4} proportionality of the nonequilibrium structure factor for large values of the magnitude q of the wave vector $\mathbf{q}$ of the fluctuations. Furthermore, we shall show that, close to the instability, there exists at least one maximum in the amplitude of nonequilibrium fluctuations, indicating that they are maximally enhanced at a particular value of the wave number q. As the critical value of the Rayleigh number is approached ($Ra \to Ra_c$), this maximum enhancement continues to increase, diverging eventually. This is precisely the cause for convective patterns to spontaneously appear above $Ra = Ra_c$, the convection threshold. Very close to the instability nonlinear effects are expected to saturate the amplitude of the nonequilibrium fluctuations and break the rotational symmetry in the wave vector $\mathbf{q}$; however, a nonlinear theory of fluctuations is outside the scope of our present treatment.

Unfortunately, in the nonequilibrium thermodynamics of mixtures there does not exist a universally agreed upon nomenclature and sign convention for some of the thermophysical properties appearing in the theory. In this paper we closely follow the recommendations made in the book edited by Köhler and Wiegand [11].

We have organized our material as follows. First, in Section 2 we present the linearized stochastic Boussinesq equations for a binary mixture as the starting point of our analysis. Next, in Section 3, we introduce the Galerkin approximation adopted for solving the stochastic Boussinesq equations with realistic boundary conditions for both temperature and concentration fluctuations. In Section 4 we then elucidate the procedure for deriving the structure factors that can be probed experimentally by shadowgraphy or small-angle light scattering. Before presenting our actual results, we consider first in Section 5 the particular case of the Boussinesq equations in thermal equilibrium. Since the exact expressions for the structure factor of a binary fluid in thermal equilibrium are well known, the thermal-equilibrium case will provide a test of the quality of the Galerkin-approximation procedure adopted. Next, in Section 6, we present the main results of our investigation: nonequilibrium temperature and concentration fluctuations are discussed and explicit analytical expressions presented. In Section 7 we develop a simple and useful expression for the nonequilibrium concentration fluctuations, taking advantage of the fact that, for common mixtures, the Lewis number is small. Our findings are summarized in Section 8.

2 Stochastic Boussinesq equations for a binary mixture

The problem of a fluid placed between two horizontal (perpendicular to gravity) plates and subjected to a stationary temperature gradient, ∇T_0, is usually referred to as the Rayleigh-Bénard (RB) problem. In the case of a binary mixture, for moderate values of the temperature gradient, a stationary concentration gradient ∇c_0 develops in the fluid, due to the Soret effect. The relationship between the stationary concentration and temperature gradients is

$$\nabla c_0 = -\bar{c}_0(1-\bar{c}_0)S_T\ \nabla T_0, \tag{1}$$

where $\bar{c}_0$ is the average stationary concentration through the layer (expressed as mass fraction of component 1 of the mixture), and S_T is the Soret coefficient of component 1 in component 2. For isotropic mixtures S_T is a scalar quantity and the concentration gradient is parallel (or antiparallel for $S_T < 0$) to the imposed temperature gradient. Both the temperature and the concentration gradients contribute to the density gradient through the thermal and solutal expansion coefficients, α and β, respectively:

$$\alpha = -\frac{1}{\rho}\left(\frac{\partial\rho}{\partial T}\right)_{c,p}, \qquad \beta = \frac{1}{\rho}\left(\frac{\partial\rho}{\partial c}\right)_{T,p}, \tag{2}$$

where ρ is the density and p the pressure, so that $\rho = \rho(p,T,c)$ is the equation of state of the mixture. Notice that β is positive when component 1 (the one chosen to define concentration) is the heavier component, while β is negative when component 1 is the lighter component of the mixture. With the definition (2), α is usually positive. The ratio between the contribution $\beta\nabla c_0$ of the concentration gradient and the contribution $-\alpha\nabla T_0$ of the temperature gradient to the density gradient is called the separation ration ψ. From equation (1) it follows that ψ may be expressed as

$$\psi = \bar{c}_0(1-\bar{c}_0)S_T\frac{\beta}{\alpha}. \tag{3}$$

It is worth noting that the sign of ψ is independent of whether component 1 is chosen to be the heavier or the lighter component of the mixture [12].

Equation (1) implies that both concentration and temperature gradients are stationary in space and in time; thus it refers to the so-called "conductive" solution of the RB problem. As is well known, the conductive solution is only stable for certain (moderate) values of the imposed temperature gradient, depending on its sign and the sign of the separation ratio. This is not the place to enter into a detailed discussion of the stability of the conductive solution in the RB problem for a binary mixture. We refer the interested reader to pertinent reviews [13–15]. However, some comments on the linear instability shall be needed at the end of Section 4. In this paper we shall be concerned with thermal fluctuations around the conductive solution. Hence, from here on, we shall assume that we are inside

the stability region of the solution (1) of the binary RB problem.

To describe fluctuations around the conductive solution we adopt, as usual, the Boussinesq approximation [16]. Additionally, we need to add to the thermodynamic dissipative fluxes a stochastic part, that accounts for the effects of the thermal noise. Consequently, we adopt as starting point of our analysis the (linearized) Boussinesq equations for a binary mixture, supplemented with random thermal-noise terms, which read [12]

$$\frac{\partial}{\partial t}\left(\nabla^2 w\right) = \nu\,\nabla^2\left(\nabla^2 w\right) + g\left(\frac{\partial^2}{\partial x^2}+\frac{\partial^2}{\partial y^2}\right)[\alpha\,\theta - \beta\,\Gamma] + \frac{1}{\rho}\left\{\nabla\times[\nabla\times(\nabla\cdot\delta\Pi)]\right\}_z, \tag{4a}$$

$$\frac{\partial\theta}{\partial t} = a\,\nabla^2\theta - w\,\nabla T_0 - \frac{a}{\lambda}\nabla(\delta\mathbf{Q}), \tag{4b}$$

$$\frac{\partial\Gamma}{\partial t} = D\left[\nabla^2\Gamma + \frac{\alpha}{\beta}\psi\,\nabla^2\theta\right] - w\nabla c_0 + \frac{\nabla(\delta\mathbf{J})}{\rho}. \tag{4c}$$

Here, $w(\mathbf{r},t)$ is the fluctuation in the velocity component parallel to the gravity at position $\mathbf{r}$ and time t: $w(\mathbf{r},t) = \delta u_z(\mathbf{r},t)$, $\theta(\mathbf{r},t) = \delta T(\mathbf{r},t)$ is the fluctuation of the local temperature from the average temperature $T_0(\mathbf{r})$, and $\Gamma(\mathbf{r},t) = \delta c(\mathbf{r},t)$ is the fluctuation of the local concentration around the average concentration $c_0(\mathbf{r})$. The symbol a represents the thermal diffusivity (also called thermometric coefficient) of the mixture, ν its kinematic viscosity, λ its thermal conductivity, D its mutual diffusion coefficient, and ρ the (average) fluid density through the layer. The symbol g represents the gravitational acceleration constant. In general for a binary mixture there are three dissipative fluxes, so the thermal noise has three components which are represented in equations (4) by $\delta\mathbf{Q}(\mathbf{r},t)$ for the random heat flux, by $\delta\Pi(\mathbf{r},t)$ for the random (deviatoric) stress tensor and by $\delta\mathbf{J}(\mathbf{r},t)$ for the random diffusion flux. Equations (4) represent the linearized Boussinesq equations for the fluctuating fields, since we are considering here only the case where the conductive solution is stable, so that fluctuations around it are expected to be small. In equation (4a) the random noise has to be identified with the Z-component of the vector between curly brackets. In this same equation (4a), by taking a double rotational and using the incompressibility condition, we show that pressure fluctuations do not couple with temperature or concentration fluctuations, or with ∇T_0, so that they may be neglected for the purpose of the present paper.

The average over fluctuations of the random dissipative fluxes is zero: $\langle\delta\mathbf{Q}(\mathbf{r},t)\rangle = \langle\delta\Pi(\mathbf{r},t)\rangle = \langle\delta\mathbf{J}(\mathbf{r},t)\rangle = 0$; consequently the "conductive" state with $w=\theta=\Gamma=0$ is a solution of the Boussinesq equations (4), when averaged over fluctuations. However, the correlation functions associated with temperature and/or concentration fluctuations, whose calculation is our goal here, are generically not zero. To calculate such quantities, we need expressions for the correlation functions among the components of the random dissipative fluxes. In applying fluctuating hydrodynamics to nonequilibrium steady states it is usually assumed that, due to the existence of local equilibrium, the correlation functions among the various components of the random dissipative fluxes are given by the same fluctuation-dissipation theorem (FDT) that yields these correlation functions in equilibrium, but where the various thermophysical properties have to be evaluated locally [17,18]. For the random stress tensor, the FDT states

$$\langle\delta\Pi_{ij}(\mathbf{r},t)\cdot\delta\Pi_{kl}(\mathbf{r}',t')\rangle = 2k_{\mathrm{B}}T\eta\,(\delta_{ik}\delta_{jl}+\delta_{il}\delta_{jk})\,\delta(\mathbf{r}-\mathbf{r}')\;\delta(t-t'), \tag{5}$$

where k_{B} is Boltzmann's constant and η the shear viscosity of the liquid. In equation (5), the incompressibility assumption (implicit in the Boussinesq approximation) was used to slightly simplify the more general expression found, for instance, in [19]. As commented before, the product $T\eta$, appearing as a prefactor in equation (5), has to be evaluated locally, so that in our case it will depend on the vertical position z. Thus, the random stress tensor in a nonequilibrium steady state will be, in principle, inhomogeneously correlated, although continuing to be spatially short ranged. As studied by several authors [20,21], inhomogeneously correlated short-ranged noise causes the fluctuations of the thermodynamic fields (temperature, concentration, ...) to become spatially long ranged. However, as we have discussed in a previous publication [22], when couplings between the fluctuating fields are present (as is the case here), the long-ranged effects resulting from the inhomogeneously correlated thermal noise are completely negligible compared with the long-ranged effects caused by the hydrodynamic couplings. Hence, we may identify all thermophysical properties in the noise correlation functions with their average value at the center of the fluid layer. Therefore, from here on, we shall identify the temperature T in the thermal-noise correlation functions with the average local temperature $\bar{T}_0$ at the center of the layer, and similarly the concentration c with $\bar{c}_0$. These assumptions are also consistent with the Boussinesq approximation.

In a binary mixture, the random heat and diffusion fluxes are coupled such that [10,23,24]:

$$\begin{aligned}
&\langle\delta Q_i(\mathbf{r},t)\cdot\delta Q_j(\mathbf{r}',t')\rangle = \\
&\qquad 2k_{\mathrm{B}}T^2\left\{\lambda + \frac{\rho D k_T^2}{T}\left(\frac{\partial\mu}{\partial c}\right)\right\}\delta_{ij}\;\delta(\mathbf{r}-\mathbf{r}')\;\delta(t-t'),\\
&\langle\delta Q_i(\mathbf{r},t)\cdot\delta J_j(\mathbf{r}',t')\rangle = 2k_{\mathrm{B}}T\rho D k_T\;\delta_{ij}\;\delta(\mathbf{r}-\mathbf{r}')\;\delta(t-t'),\\
&\langle\delta J_i(\mathbf{r},t)\cdot\delta J_j(\mathbf{r}',t')\rangle = \\
&\qquad 2k_{\mathrm{B}}T\rho D\left(\frac{\partial\mu}{\partial c}\right)^{-1}\;\delta_{ij}\;\delta(\mathbf{r}-\mathbf{r}')\;\delta(t-t'),
\end{aligned} \tag{6}$$

where, as noted before, all thermophysical properties appearing as prefactors will be evaluated at the center of the layer: *i.e.*, $T=\bar{T}_0$. In equation (6), μ represents the difference between the chemical potential of component 1 and the chemical potential of component 2 (both chemical potentials are taken per unit mass, so that the SI unit for μ is J kg^{-1}). Of course, the concentration derivative of μ

$$\mathcal{H}(\omega,q)=\begin{bmatrix} \mathrm{i}\omega(q^2-\partial_z^2)+\nu(q^2-\partial_z^2)^2 & -\alpha g q^2(1+\psi) & g q^2 \\ \nabla T_0 & \mathrm{i}\omega+a(q^2-\partial_z^2) & 0 \\ -\alpha\psi\ \nabla T_0 & -\alpha\psi\ \mathrm{i}\omega & \mathrm{i}\omega+D(q^2-\partial_z^2) \end{bmatrix} \tag{11}$$

is also to be evaluated at the center of the layer. Additionally, when applying equations (5) and (6), we shall neglect the Dufour effect ($k_T = 0$), so that the cross-correlation between random dissipative heat and diffusion flows will be neglected here [24]. This is a good approximation for liquids, while for gases the Dufour effect should not be neglected [24].

To complete the working equations for this paper, we consider next the boundary conditions. The physically realistic boundary conditions for our problem are rigid and impermeable walls [9,14,24]:

$$w=\partial_z w=\theta=\partial_z(\beta\Gamma+\psi\alpha\theta)=0, \quad \text{at } z=\pm\tfrac{1}{2}L. \tag{7}$$

The last condition ensures that the solute flux vanishes at the walls, including the solute transport due to the Soret effect. When comparing with the work of some previous investigators [9,24], one should recall that we use here the definition (3) of the separation ratio ψ recommended in the book edited by Köhler and Wiegand [11].

In view of the last of the boundary conditions (7), it is convenient to use, instead of Γ, the dimensionless variable $\zeta=\beta\Gamma+\psi\alpha\theta$, so that the stochastic binary Boussinesq equations now read

$$\frac{\partial}{\partial t}\left(\nabla^2 w\right)=\nu\nabla^2\left(\nabla^2 w\right) +g\ \left(\partial_x^2+\partial_y^2\right)\left[(1+\psi)\alpha\theta-\zeta\right]+F_1, \tag{8a}$$

$$\frac{\partial\theta}{\partial t}=a\nabla^2\theta-w\ \nabla T_0+F_2, \tag{8b}$$

$$\frac{\partial\zeta}{\partial t}=D\nabla^2\zeta+\alpha\psi\frac{\partial\theta}{\partial t}+w\ \alpha\psi\nabla T_0+F_3, \tag{8c}$$

where, to shorten the notation, we have introduced spatiotemporal Langevin random-noise terms as

$$F_1(\mathbf{r},t)=-\frac{1}{\rho}\left\{\nabla\times\left[\nabla\times\left(\nabla\cdot\delta\Pi(\mathbf{r},t)\right)\right]\right\}_z,$$
$$F_2(\mathbf{r},t)=-\frac{a}{\lambda}\ \nabla\delta\mathbf{Q}(\mathbf{r},t), \qquad F_3(\mathbf{r},t)=\frac{\beta}{\rho}\ \nabla\delta\mathbf{J}(\mathbf{r},T). \tag{9}$$

The correlation functions between these three random-noise terms may be deduced from the FDT, equations (5-6), and will be discussed later.

3 Galerkin approximation for the calculation of the fluctuating fields

To solve the set of equations (8) for the fluctuating fields while accommodating the boundary conditions in the Z-direction, as usual [6,17,25], we apply a Fourier transform in time and in the horizontal XY-plane, reducing equations (8) to

$$\mathcal{H}(\omega,q)\cdot\begin{bmatrix} w(z,\omega,\mathbf{q}) \\ \theta(z,\omega,\mathbf{q}) \\ \zeta(z,\omega,\mathbf{q}) \end{bmatrix}=\begin{bmatrix} F_1(z,\omega,\mathbf{q}) \\ F_2(z,\omega,\mathbf{q}) \\ F_3(z,\omega,\mathbf{q}) \end{bmatrix}, \tag{10}$$

where $\mathcal{H}(\omega,q)$ is a (linear) hydrodynamic operator

see equation (11) *above.*

In equations (10) and (11), ω and $\mathbf{q}$ are the Fourier variables, representing the frequency and the (horizontal) wave vector of the fluctuations, respectively. In some previous publications [6,25,26] we used the notation $q_\parallel$, to emphasize that $\mathbf{q}$ is a two-dimensional vector in the horizontal plane. In this paper we do not use this notation, since all vectors appearing in the present paper will be in the horizontal plane.

In equations (10) and (11), we have reduced our problem to solving a system of ordinary linear differential equations, subjected to the boundary conditions (7) at $z=\pm\frac{1}{2}L$. This can only be performed analytically by some approximation method. For fitting or analyzing experimental data, analytical expressions, though approximate, are very useful. Here we adopt a Galerkin-approximation method, since it has yielded good results in the case of the Boussinesq equations for a pure fluid with realistic boundary conditions [6,27]. For the binary mixture under consideration here, we adopt the same Galerkin test functions previously employed by Lhost *et al.* [9] with excellent results, for performing a linear stability analysis. Hence, we look for approximate solutions to equations (9-10) whose z-dependence may be expressed in the form:

$$\begin{aligned} w(z,\omega,\mathbf{q})&=w_0(\omega,\mathbf{q})\ \mathcal{C}_1(z),\\ \theta(z,\omega,\mathbf{q})&=\theta_0(\omega,\mathbf{q})\ \sqrt{2}\ \cos\frac{\pi z}{L},\\ \zeta(z,\omega,\mathbf{q})&=\zeta_0(\omega,\mathbf{q})\ 1, \end{aligned} \tag{12}$$

where $\mathcal{C}_1(z)$ is the function

$$\mathcal{C}_1(z)=\frac{\cosh(\Lambda z/L)}{\cosh(\Lambda/2)}-\frac{\cos(\Lambda z/L)}{\cos(\Lambda/2)}, \tag{13}$$

with, $\Lambda\approx 4.73$, corresponding to the first Chandrasekhar function. This value of Λ assures that the derivative of $\mathcal{C}_1(z)$ vanishes at $z=\pm\frac{1}{2}L$ [16]. Consequently, the set of test functions (12) satisfies the required boundary conditions (7).

Substituting equations (12) into equations (10-11), and projecting the first of the expressions obtained by such

substitution onto the first Galerkin function $\mathcal{C}_1(z)$, further projecting the second of the expressions onto the second Galerkin function $\sqrt{2}\cos\pi z/L$, and similarly for the third, we arrive at the following set of algebraic equations for the amplitudes:

$$\mathsf{A}(\omega,q)\cdot\begin{pmatrix} w_0(\omega,\mathbf{q}) \\ \theta_0(\omega,\mathbf{q}) \\ \zeta_0(\omega,\mathbf{q})\end{pmatrix} = \begin{pmatrix} F_1(\omega,\mathbf{q}) \\ F_2(\omega,\mathbf{q}) \\ F_3(\omega,\mathbf{q})\end{pmatrix}, \tag{14}$$

with the matrix $\mathsf{A}(\omega,q)$ given by

$$\mathsf{A}(\omega,q) = \begin{bmatrix} \mathrm{i}\omega\frac{A(q)}{L^2}+\nu\frac{B(q)}{L^4} & -\alpha g q^2(1+\psi)P_1 & P_0 g q^2 \\ P_1\nabla T_0 & \mathrm{i}\omega + aq^2C_1(q) & 0 \\ -P_0\alpha\psi\nabla T_0 & -\alpha\psi\frac{2\sqrt{2}}{\pi}\ \mathrm{i}\omega & \mathrm{i}\omega + D\ q^2\end{bmatrix}. \tag{15}$$

In equation (15) for $\mathsf{A}(\omega,q)$, the various dimensionless projections of the Galerkin test functions are

$$P_0 = \frac{1}{L}\int_{-L/2}^{L/2}\mathrm{d}z\ \mathcal{C}_1(z) = \frac{4}{\Lambda}\tanh\left(\tfrac{\Lambda}{2}\right), \tag{16}$$

$$P_1 = \frac{1}{L}\int_{-L/2}^{L/2}\mathrm{d}z\ \sqrt{2}\cos\left(\frac{\pi z}{L}\right)\ \mathcal{C}_1(z) = \frac{4\sqrt{2}\pi\Lambda^2}{\Lambda^4-\pi^4}, \tag{17}$$

$$A(q) = L\int_{-L/2}^{L/2}\mathrm{d}z\ \mathcal{C}_1(z)\left\{[q^2-\partial_z^2]\cdot\mathcal{C}_1(z)\right\} = q^2L^2 + \frac{P_0\Lambda^2}{16}\left(P_0\Lambda^2-8\right) = \tilde{q}^2 + P_2\Lambda^2, \tag{18}$$

and, finally,

$$B(q) = L^3\int_{-L/2}^{L/2}\mathrm{d}z\ \mathcal{C}_1(z)\left\{[q^2-\partial_z^2]^2\cdot\mathcal{C}_1(z)\right\} = \tilde{q}^4 + \frac{P_0\Lambda^2}{8}\left(P_0\Lambda^2-8\right)\tilde{q}^2 + \Lambda^4 = A^2(\tilde{q}) + \Lambda^4(1-P_2^2), \tag{19}$$

with

$$P_2 = \frac{P_0}{16}(P_0\Lambda^2-8). \tag{20}$$

In equations (16) to (19), $\tilde{q}=qL$ is the dimensionless wave number of the fluctuations. The additional dimensionless function $C_1(q)$ introduced in equation (15), will be defined in equation (33) below. It is worth noting for future use, that both $A(q)$ and $B(q)$ depend only on the magnitude $\tilde{q}$ of the dimensionless vector $\tilde{\mathbf{q}}$, being always real and positive valued functions. Finally, the random forces $F_1(\omega,\mathbf{q})$, etc., appearing in equation (14) are the projections onto the Galerkin test functions of the corresponding Langevin random-noise terms (9), so that

$$F_1(\omega,\mathbf{q}) = \frac{1}{L}\int_{-L/2}^{L/2}\mathrm{d}z\ F_1(z,\omega,\mathbf{q})\ \mathcal{C}_1(z), \quad \text{etc.} \tag{21}$$

Inverting the matrix in equation (15), we immediately solve for the amplitudes of the fluctuations: $w_0(\omega,q)$, etc. To calculate the correlation functions among the various fluctuating fields, we do need the correlations among the projections of the Langevin noise terms introduced in equation (21). They can be computed from their definition, equation (21), the relationship between Langevin noise and random dissipative fluxes, equations (9), and the FDT for a binary mixture, equations (5) and (6). The resulting correlation functions are conveniently expressed in terms of a correlation matrix, $\mathsf{C}(q)$, defined by

$$\langle F_i(\omega,\mathbf{q})F_j^*(\omega',\mathbf{q}')\rangle = (2\pi)^3\ C_{ij}(q)\ \delta(\mathbf{q}-\mathbf{q}')\ \delta(\omega-\omega'). \tag{22}$$

Following the guidelines above, we have evaluated the correlation matrix as

$$\mathsf{C}(q) = \frac{2k_{\mathrm{B}}T}{\rho L^5}\begin{bmatrix}\nu q^2B(q) & 0 & 0 \\ 0 & aq^2C_1(q)\ \xi_2 & 0 \\ 0 & 0 & Dq^2\xi_3\end{bmatrix}, \tag{23}$$

where $B(q)$ is the same function defined by equation (19). The parameters ξ_2 and ξ_3 give the relative strength of the various components of the noise:

$$\xi_2 = \frac{L^4T}{c_p}, \qquad \xi_3 = L^4\beta^2\left(\frac{\partial\tilde{\mu}}{\partial c}\right)^{-1}_{p,T}. \tag{24}$$

Recall that, in deducing equation (23), we have neglected the Dufour effect in the FDT (6), and we have evaluated all thermophysical properties at their average values in the layer. The current calculation is similar, though more involved, to calculations performed in previous work [6, 27], where the interested reader may find more details.

4 Evaluation of nonequilibrium structure factors

The information in the previous section provides us with all the ingredients required to calculate the two-point equal-time correlation functions among the various nonequilibrium fluctuating fields, which is our final goal. It turns out that all such correlation functions have a similar mathematical structure, which is best illustrated for the temperature-fluctuations autocorrelation function, which can be expressed as

$$\langle\theta(\mathbf{q},z,t)\cdot\theta^*(\mathbf{q}',z',t)\rangle = (2\pi)^2\ \delta(\mathbf{q}-\mathbf{q}') \times\int_{-\infty}^{\infty}\mathrm{d}\omega\ S_{\theta\theta}(\omega,q)2\cos(\pi z/L)\ \cos(\pi z'/L), \tag{25}$$

where $S_{\theta\theta}(\omega,q)$ is a dynamic structure factor associated with temperature fluctuations. From the theory developed in the previous section, such a dynamic structure factor for the temperature fluctuations may be expressed as

$$S_{\theta\theta}(\omega,q) = \left[\mathsf{A}^{-1}(\omega,q)\right]_{2i}\left[\mathsf{A}^{-1*}(\omega,q)\right]_{2j}C_{ij}(q), \tag{26}$$

with the matrix $\mathsf{A}(\omega,q)$ as defined in equation (15). Equation (26) includes a summation over the (coordinate) indices i and j. The index 2 appears in the components of

$\mathsf{A}(\omega, q)$ because temperature is the second component in the vector of fluctuating fields, as defined by equation (10). The integration over ω appears in equation (25) because we are applying a double inverse Fourier transform in ω and ω', and the two-frequencies correlation function turns out to be proportional to $\delta(\omega - \omega')$, as can be easily shown from equation (22).

The other equal-time correlation functions among the fluctuating fields have a structure similar to equation (25): they are proportional to delta-functions $\delta(\mathbf{q} - \mathbf{q}')$, while the product of two Galerkin test functions represents the dependence on z and z'. The dependence on ω and q can always be encapsulated in a corresponding "dynamic structure factor", like the one defined in equation (26). For instance, similarly to equation (26) for temperature fluctuations, it is possible to define a dynamic structure factor for the fluctuations in the ζ-variable as

$$S_{\zeta\zeta}(\omega, q) = \left[\mathsf{A}^{-1}(\omega, q)\right]_{3i} \left[\mathsf{A}^{-1*}(\omega, q)\right]_{3j} C_{ij}(q). \quad (27)$$

The main goal of the present paper is the calculation of the structure factor that it is probed by shadowgraph or light scattering experiments. As discussed elsewhere [2,6, 28], the various contributions to the experimental structure factor, are obtained by integration over the vertical variables, z and z', of the equal-time correlation functions between fluctuating fields. For instance, the autocorrelation function of the temperature fluctuations contributes to the experimental structure factor a term proportional to $S_{\theta\theta}(q)$, defined by

$$(2\pi)^2\ S_{\theta\theta}(q)\ \delta(\mathbf{q} - \mathbf{q}') = \frac{1}{L}\int_{-L/2}^{L/2} \mathrm{d}z \int_{-L/2}^{L/2} \mathrm{d}z'\ \langle \theta(\mathbf{q}, z, t) \cdot \theta^*(\mathbf{q}', z', t)\rangle. \quad (28)$$

Note that the dimension of $S_{\theta\theta}(q)$ in equation (28) is temperature square times volume. In addition to equation (28) for $S_{\theta\theta}(q)$, there are similar contributions to the experimental structure factor arising from the ζ fluctuations, $S_{\zeta\zeta}(q)$, as well as from the cross-correlation between temperature and ζ fluctuations, $S_{\zeta\theta}(q)$. For these other contributions, the double spatial integral in equation (28) will be over the corresponding Galerkin test functions, instead of the temperature-fluctuations ones displayed in equation (25). Further comments about the validity of equation (28), when a Hopf bifurcation is present in the system, will be made at the beginning of Section 6.

The calculation of $S_{\theta\theta}(q)$ and the other contributions to the experimental structure factor are quite straightforward, but they require a lot of algebra. The most complicated item is the expression for the inverse matrix $\mathsf{A}^{-1}(\omega, q)$, which involves the inverse of the determinant of $\mathsf{A}(\omega, q)$. If, following previous authors [9], we use a dimensionless frequency defined by $\tilde{\omega} = (L^2/a)\ \omega$, then such determinant may be expressed as a cubic polynomial in the dimensionless variable $\tilde{\omega}$:

$$|\mathsf{A}(\omega, q)| = \frac{a^3}{L^8}\{-\mathrm{i}\ A(q)\ \tilde{\omega}^3 - B(q)D_1(q)\ \tilde{\omega}^2 + \mathrm{i}Pr\ \tilde{q}^2 B(q)C_5(q, Ra)\ \tilde{\omega} + PrLe\ \tilde{q}^4 B(q)C_1(q)D_2(q, Ra)\}, \quad (29)$$

where we have introduced several dimensionless functions:

$$D_1(q) = Pr + \frac{Le + C_1(q)}{C_2(q)}, \quad (30a)$$

$$C_5(q, Ra) = P_1^2 C_4(q) - \frac{Le^2}{PrC_2(q)} - \frac{P_1^2(1 + P_3\psi)Ra}{B(q)}, \quad (30b)$$

$$D_2(q, Ra) = 1 - \frac{P_1^2[1 + C_3(q)\psi]Ra}{C_1(q)B(q)}. \quad (30c)$$

In equations (29-30), Ra is the dimensionless Rayleigh number, defined as

$$Ra = -\frac{\alpha g L^4 \nabla T_0}{a\nu}, \quad (31)$$

while $Pr = \nu/a$ and $Le = D/a$ are the dimensionless Prandtl and Lewis numbers, respectively. The function $B(q)$ was previously defined in equation (19). The dimensionless parameter P_3 appearing in equation (30b) is given by

$$P_3 = 1 + \frac{P_0^2}{P_1^2} - \frac{2P_0\sqrt{2}}{\pi P_1} \approx 0.951. \quad (32)$$

Furthermore, following [9], we have introduced in equations (30) some functions that will be useful in the remainder of this paper. They are

$$C_1(q) = \frac{\tilde{q}^2 + \pi^2}{\tilde{q}^2}, \qquad C_2(q) = \frac{B(q)}{\tilde{q}^2 A(q)}, \quad (33a)$$

and

$$C_3(q) = 1 + \frac{P_0^2 C_1(q)}{P_1^2 Le}, \quad (33b)$$

$$C_4(q) = \frac{[Pr\ C_2(q) + Le][C_1(q) + Le]}{Pr\ P_1^2 C_2(q)}, \quad (33c)$$

where $\tilde{q} = qL$ is again the dimensionless wave number. It is worth noting that, in the limit $q \to \infty$, both $C_1(q)$ and $C_2(q)$ reach the limiting value unity, while they diverge proportionally to q^{-2} in the limit $q \to 0$. By substituting equations (33) into equations (30), it may be observed that all four C functions have similar asymptotic behaviors: they reach a finite limit as $\tilde{q} \to \infty$, while they diverge proportionally to $\tilde{q}^{-2}$ as $\tilde{q} \to 0$. The four C functions are monotonically decreasing functions of q, always positive, reaching the minimum at the limit $q \to \infty$. However, the D functions reach finite limits at both $\tilde{q} \to \infty$ and $\tilde{q} \to 0$.

The next step in the calculation of $\mathsf{A}^{-1}(\omega, q)$, as usual, consists in expressing the determinant (29) of the matrix $\mathsf{A}(\omega, q)$ in terms of its three complex $\tilde{\omega}$-roots:

$$|\mathsf{A}(\tilde{\omega}, q)| = A(q)\ [\mathrm{i}\ \tilde{\omega} - \Omega_1(q)][\mathrm{i}\ \tilde{\omega} - \Omega_2(q)][\mathrm{i}\ \tilde{\omega} - \Omega_3(q)]. \tag{34}$$

The roots $\Omega_1(q)$, $\Omega_2(q)$ and $\Omega_3(q)$ correspond to the three different decay rates of the thermodynamic fluctuations in a binary mixture [29]. Explicit expressions may be obtained from the formulas for the roots of a cubic equation, but the resulting expressions are complicated and will not be discussed here. Moreover, they are not actually required, since we focus here on the intensity (equal-time correlation functions, obtained by integration over ω), and not on the dynamics of the fluctuations; see equations (25) and (28). Traditionally, shadowgraph experiments have been employed to study the intensity of the fluctuations [1, 28]. However, more recently [2], the shadowgraph technique has been extended to yield also some information regarding the dynamics of the fluctuations. For the latter purpose, explicit knowledge of the decay rates $\Omega_i(q)$ will be required.

The ω-integration in equations (25) and (28) for the calculation of the (static) structure factor is convergent only if the real part of the three decay rates $\Omega_i(q)$ is nonzero for all values of q. Hence, as already found in previous publications for the case of a one-component fluid [6, 25], the conditions under which it is possible to calculate a static structure factor ($S_{\theta\theta}(q)$ for temperature fluctuations, or any other) can be determined from a classical linear stability analysis [16]. For the problem considered here, a detailed linear instability analysis was already performed by Lhost *et al.* [9], who used the same set of Galerkin test functions. We simply mention that, looking back at equation (29), we can easily see that one possibility for having a decay rate with zero real part is $D_2(q) = 0$, which happens when $Ra = R_\mathrm{s}(\tilde{q})$, with the function $R_\mathrm{s}(\tilde{q})$ defined by

$$R_\mathrm{s}(\tilde{q}) = \frac{(\tilde{q}^2 + \pi^2)}{P_1^2 \tilde{q}^2} \frac{(\tilde{q}^2 + P_2 \Lambda^2)^2 + \Lambda^4 (1 - P_2^2)}{1 + \left[1 + \dfrac{P_0^2 (\tilde{q}^2 + \pi^2)}{P_1^2 \tilde{q}^2 Le}\right] \psi}. \tag{35}$$

The condition $Ra = R_\mathrm{s}(\tilde{q})$, with $R_\mathrm{s}(\tilde{q})$ given by equation (35), reproduces exactly equation (7) in reference [9] for the I_s stationary instability of the binary Boussinesq problem. In fact, when condition (35) holds, $\Omega_0(q) = 0$ is a root of the determinant (29), both real and imaginary parts being zero. Thus, the corresponding instability is stationary indeed. Looking for the minimum as a function of $\tilde{q}$ of equation (35), the critical wave number for the stationary instability, $\tilde{q}_\mathrm{c,s}$, may be calculated. The corresponding critical Rayleigh number is then obtained by evaluating equation (35) at the minimum: $Ra_\mathrm{c,s} = R_\mathrm{s}(\tilde{q}_\mathrm{c,s})$. Depending on the values of ψ and Le, the critical wave number may be both zero or nonzero, though for usual binary mixtures $\tilde{q}_\mathrm{c,s} \neq 0$. However, for $\psi > 0$, $Ra_\mathrm{c,s}$ is always positive [9]. Explicit analytical expressions of such critical values result quite involved, so that they are usually discussed numerically, as extensively done by Lhost *et al.* [9]. We should also mention that, by setting $\psi = 0$ in equation (35) we recover previous results obtained by Niederländer *et al.* [30] for the first convective instability in a one-component fluid.

As discussed in more detail by Lhost *et al.* [9], there is another possibility for one of the ω-roots of $|\mathsf{A}(\omega, q)|$ having zero real part, namely: $D_1(q)C_5(q, Ra) - Le\ C_1(q)\ D_2(q, Ra)/C_2(q) = 0$. In this case, it may be easily verified that $\Omega_0(q) = \mathrm{i}\ D_1(q)B(q)/A(q)$ is a root of $|\mathsf{A}(\omega, q)|$, with a zero real part, but a nonzero imaginary part. Thus, the corresponding instability is oscillatory, or Hopf-like. The condition for the oscillatory I_o instability, similarly to the I_s instability, can be expressed as $Ra = R_\mathrm{o}(\tilde{q})$, where

$$R_\mathrm{o}(\tilde{q}) = \frac{B(q)C_4(q)}{[1 + D_3(q)\psi]}, \tag{36}$$

with

$$D_3(q) = P_3 - \frac{P_0^2}{P_1^2} + \frac{Pr\ P_0^2 C_2(q) + P_1^2 Le(P_3 - 1)}{P_1^2[Pr\ C_2(q) + C_1(q)]}. \tag{37}$$

The function $D_3(q)$ has finite limits at both $q \to \infty$ and $q \to 0$, as had the two D functions introduced previously. The condition $Ra = R_\mathrm{o}(\tilde{q})$, with $R_\mathrm{o}(\tilde{q})$ given by equation (36) with the appropriate change of notation, reproduces the result reported by Lhost *et al.* [9], who used the same set of Galerkin test functions. Looking for the minimum value of $R_\mathrm{o}(\tilde{q})$ (as a function of $\tilde{q}$) in equation (36), the critical Rayleigh number for the Hopf bifurcation, $Ra_\mathrm{c,o}$, may be evaluated. It turns out that, for $\psi > 0$, $Ra_\mathrm{c,o} > Ra_\mathrm{c,s}$, while for $\psi < 0$, $Ra_\mathrm{c,o} > Ra_\mathrm{c,s}$ [9]. Thus, the Rayleigh instability is critical for mixtures with positive separation ratios, while for negative separation ratios the Rayleigh instability is subcritical, and the Hopf instability critical. The presence of these two competing instability mechanisms is important for the physical interpretation of the nonequilibrium fluctuations, as will be discussed in more detail in Section 6. For future use it should be noticed that the two functions $R_\mathrm{s}(q)$ and $R_\mathrm{o}(q)$ become proportional to q^4 in the limit of large q. For $q \to 0$, $R_\mathrm{o}(q) \propto q^{-2}$, while $R_\mathrm{s}(q)$ reaches a finite limit.

We conclude this section by pointing out that, from equations (35) and (36), one finds a fairly good approximations for the critical Rayleigh and wave numbers [9]. For instance, the fact that the stationary instability happens first for positive ψ while the oscillatory instability happens first for negative ψ, is known to be exactly correct [14]. These facts give us confidence in the adequacy of the Galerkin-approximation procedure (12). Further evidence for the quality of the Galerkin test functions (12) is presented in the next section.

5 Structure factor in thermal equilibrium

The structure factor of a binary liquid mixture in thermal equilibrium is well known, so that we can use this limit to test the quality of our Galerkin approximation, equation (12). It is the goal of the present section to perform such a test. In equilibrium the correlation functions

become spatially short ranged, so that they may be calculated without taking into account any boundary conditions. Hence, they can be simply evaluated [29,31] by performing a full spatiotemporal Fourier transform (including the direction of the gravity, perpendicular to the bounding plates) of the original binary Boussinesq equations (8) with $\nabla T_0 = 0$. In this way we readily obtain, for instance, the autocorrelation function of the temperature fluctuations as [29,31]

$$\langle \theta(\omega, \mathbf{q}) \cdot \theta^*(\omega', \mathbf{q}') \rangle = \frac{k_\mathrm{B} T^2}{\rho c_p} \frac{2aq^2}{\omega^2 + a^2 q^4} \times (2\pi)^4 \, \delta(\mathbf{q} - \mathbf{q}') \, \delta(\omega - \omega'), \quad (38)$$

where in this case $\mathbf{q}$ represents a 3-dimensional wave vector of the fluctuations, with magnitude q[1]. To evaluate the equilibrium structure factor measured in experiments, in accordance with equation (28), we need to first integrate over ω, then apply inverse Fourier transforms in z and z', and finally integrate over these two variables. We then obtain

$$S^\mathrm{E}_{\theta\theta} = \frac{k_\mathrm{B} T^2}{\rho c_p}, \quad (39)$$

where the upper index "E" denotes equilibrium. For the concentration fluctuations ($\Gamma = \beta^{-1}[\zeta - \psi\alpha\theta]$) we obtain similarly

$$S^\mathrm{E}_{\Gamma\Gamma} = \frac{k_\mathrm{B} T}{\rho} \left(\frac{\partial \mu}{\partial c} \right)^{-1}_{p,T} \left\{ 1 + \frac{Le \, \mathcal{R}_D}{(Le + 1)} \right\}, \quad (40)$$

where $\mathcal{R}_D$ is the dimensionless ratio between the strengths of the random heat flux and of the random diffusion flux:

$$\mathcal{R}_D = \frac{\alpha^2 \psi^2 \xi_2}{\xi_3} = \frac{T}{c_p} \, [c(1-c) S_T]^2 \left(\frac{\partial \mu}{\partial c} \right)_{p,T}. \quad (41)$$

Recall that μ is the difference in chemical potentials per unit mass, and c_p is also defined per unit mass, so that $\mathcal{R}_D$ is a dimensionless ratio indeed. Then, $S^\mathrm{E}_{\theta\theta}$ has indeed dimension of temperature square times volume, as already noted after equation (28), while $S^\mathrm{E}_{\Gamma\Gamma}$ has, correspondingly, dimension of volume. Notice also in equations (39) and (40) that both $S^\mathrm{E}_{\theta\theta}$ and $S^\mathrm{E}_{\Gamma\Gamma}$ do not depend on q, confirming the fact that fluctuations in equilibrium are spatially short ranged. When $\xi_3 = 0$ and $\psi = 0$ (limit of a one-component fluid), as expected, the concentration fluctuations vanish. In the case $Le \to 0$, the stochastic heat flow (whose strength is proportional to ξ_2) does not contribute to the concentration fluctuations.

As mentioned earlier, to test the quality of the test functions introduced in equation (12), we can compare the exact results, given by equations (39) and (40), with what we obtain from the Galerkin approximation for the particular case of thermal equilibrium. For this purpose, we substitute $\nabla T_0 = 0$ into equation (15) for $\mathsf{A}(\omega, q)$, we invert the resulting matrix and we calculate both $S^\mathrm{E}_{\theta\theta}(q)$ and $S^\mathrm{E}_{\Gamma\Gamma}(q)$, obtaining:

$$S^\mathrm{E}_{\theta\theta} = \frac{2k_\mathrm{B} T}{\rho L^5} \frac{4\xi_2 L}{\pi^2} = \frac{8}{\pi^2} \frac{k_\mathrm{B} T^2}{\rho c_p}, \quad (42a)$$

$$S^\mathrm{E}_{\Gamma\Gamma}(q) = \frac{k_\mathrm{B} T \xi_3}{\rho \beta^2 L^4} \left[1 + \mathcal{R}_D \frac{Le + C_1(\tilde{q}) \left(1 - \frac{8}{\pi^2}\right)}{Le + C_1(\tilde{q})} \right], \quad (42b)$$

to be compared with the expected equilibrium results (39) and (40), respectively. We first observe that equation (42a) for $S^\mathrm{E}_{\theta\theta}$ does not depend on q, as was the case for the exact structureless result (39). The temperature fluctuations within the Galerkin approximation are again short ranged (do not depend on q) and, thus, have the same qualitative behavior as the exact result. However, we find the magnitude of the temperature fluctuations obtained with the Galerkin approximation (12) is 19% smaller than the rigorous result (39). This is a shortcoming of the single-mode Galerkin approximation. Nevertheless, since the difference is not very large, the result supports the adequacy of the Galerkin test functions (12) for the calculation of the temperature fluctuations.

On the other hand, we observe in equation (42b) for $S^\mathrm{E}_{\Gamma\Gamma}$ some q-dependence, implying that we obtain some structure in equilibrium, which is an unphysical result. This is an evident shortcoming of our Galerkin approximation (12). However, from a more detailed comparison between equations (42b) and (40), we note that, on the one hand, the denominator of equation (42b) contains, instead of 1, a function of q which rapidly approaches unity for large q. Moreover, the numerator contains the same function $C_1(q)$ multiplied by a geometric factor $(1 - 8/\pi^2)$ which is very close to zero. Thus, the difference is not very important quantitatively.

Another evident shortcoming of equation (42b) is that, in the limit $Le \to 0$, the stochastic heat flow (ξ_2) yields a nonzero contribution to the concentration fluctuations, which again is an unphysical result (cf., Eq. (40)). In spite of this second shortcoming, we shall show in Section 7 that, for the nonequilibrium enhancement of concentration fluctuations, *i.e.*, when the unphysical equilibrium contribution (42b) is subtracted, a systematic $Le \to 0$ expansion produces realistic results. We conclude, from the analysis of this section, that the Galerkin approximation (12) gives a reasonable qualitative description of the structure factor, although the results are several percents off quantitatively.

6 Nonequilibrium fluctuations for $\psi > 0$

After having considered the quality of our Galerkin approximation (12), we shall evaluate and discuss the various nonequilibrium static correlation functions following the procedure described in Section 4. The present section contains the main results of our investigation.

In previous publications dealing with a one-component fluid where a Rayleigh stationary bifurcation is the only instability mechanism, the consequences for shadowgraph

[1] This is the only place in the present paper, where q represents the magnitude of a three-dimensional vector.

or light scattering experiments of the presence of long-ranged nonequilibrium fluctuations have been discussed in detail [2,28]. In particular, it was demonstrated that experimental structure factors are proportional to the result obtained upon double integration in z and z' of the equal-time thermodynamic correlation functions as stated by equation (28). In the case of a binary mixture, the situations is complicated by the presence of an oscillatory Hopf instability. When $\psi > 0$, the preferred instability mechanism continues to be stationary [9,14]. Therefore, we believe that the conclusions of previous investigations regarding the relationship between experimental structure factor and equal-time autocorrelation functions continue to hold for $\psi > 0$. For $\psi < 0$, initially, we do not see any reason why experimental structure factor should not be still obtained as in equation (28), even when the oscillatory instability is the dominant mechanism. However, this case may need further clarification, since light scattering and shadowgraph experiments always require a detailed discussion of what is actually measured (geometry of scattering volumes, mode propagation, etc.). Consequently, the conclusions in this section are intended mainly for the case $\psi > 0$, while for the case $\psi < 0$ our present results have to be considered as only provisional.

When one calculates the experimental structure factor following the steps described in Section 4, it turns out that all contributions have a similar mathematical structure, which we shall now discuss for the fluctuations of ζ. Substituting equation (27) into the equivalent of equation (28), we find that the amplitude (28) of the equal-time nonequilibrium ζ fluctuations may be cast in the form

$$S_{\zeta\zeta}(\tilde{q}) = S^{\mathrm{E}}_{\zeta\zeta}(\tilde{q}) + Ra\ S^{\mathrm{NE}}_{\zeta\zeta}(\tilde{q}, Ra), \tag{43}$$

where $S^{\mathrm{E}}_{\zeta\zeta}(\tilde{q})$ represents the same equilibrium contribution appearing in Section 5 as a contribution to $S^{\mathrm{E}}_{\Gamma\Gamma}(\tilde{q})$, while the product $Ra\ S^{\mathrm{NE}}_{\zeta\zeta}(\tilde{q}, Ra)$ is to be interpreted as the amplitude of nonequilibrium ζ fluctuations. This nonequilibrium amplitude, in turn, may be decomposed as

$$S^{\mathrm{NE}}_{\zeta\zeta}(\tilde{q}, Ra) = \frac{S^{(\mathrm{s})}_{\zeta\zeta}(\tilde{q}, Ra)}{1 - \dfrac{Ra}{R_{\mathrm{s}}(\tilde{q})}} + \frac{S^{(\mathrm{o})}_{\zeta\zeta}(\tilde{q}, Ra)}{1 - \dfrac{Ra}{R_{\mathrm{o}}(\tilde{q})}}. \tag{44}$$

In the denominators of the two terms in the LHS of equation (44), we identify the corresponding (linear) instability conditions as those earlier specified by equations (35) and (36). Therefore, we physically interpret $S^{(\mathrm{s})}_{\zeta\zeta}(\tilde{q}, Ra)$ as representing the contribution of nonequilibrium ζ fluctuations that can be associated with the stationary (Rayleigh) instability, while $S^{(\mathrm{o})}_{\zeta\zeta}(\tilde{q}, Ra)$ represents the contribution of nonequilibrium ζ fluctuations that can be associated with the oscillatory (Hopf) instability. We observe how both instability mechanisms cooperate to cause an enhancement of the fluctuations when a binary mixture is driven outside equilibrium. As will be discussed later, for the case of temperature fluctuations, a set of equations with the same structure as equations (43) and (44) is obtained, with the equilibrium contribution in (43) replaced by the corresponding $S^{\mathrm{E}}_{\theta\theta}$ and where we can identify two nonequilibrium amplitudes $S^{(\mathrm{s})}_{\theta\theta}(\tilde{q}, Ra)$ and $S^{(\mathrm{o})}_{\theta\theta}(\tilde{q}, Ra)$ associated with the stationary and with the oscillatory instability, respectively.

In addition, we recall from Section 2 that the Rayleigh instability appears when the first denominator in equation (44) vanishes, while the Hopf instability appears when the second denominator vanishes. We encounter again that (linear) instabilities correspond to divergences in a (linear) theory of nonequilibrium fluctuations, as was extensively discussed for a one-component fluid [6,25,26]. We additionally remark that all fluctuations (velocity, temperature and concentration) diverge for the same value of Ra.

Equations (43) and (44) are a compact and convenient way of expressing the various nonequilibrium static structure factors in general, allowing a clear and simple physical interpretation. We next shall discuss more extensively the particular cases of temperature and concentration fluctuations, giving explicit expressions for the amplitudes of the stationary and oscillatory nonequilibrium fluctuations in each case.

6.1 Temperature fluctuations

Substituting equation (26) into equation (28) and performing the various integrations, we obtain an expression with a structure similar to equation (43), namely:

$$S_{\theta\theta}(\tilde{q}) = S^{\mathrm{E}}_{\theta\theta}\left\{1 + \frac{C_2(\tilde{q})Pr\ \tilde{F}_{\mathrm{NE}}(\tilde{q}, Ra)}{PrC_2(\tilde{q}) + C_1(\tilde{q})}\ Ra\right\}, \tag{45}$$

with $S^{\mathrm{E}}_{\theta\theta}$ given by equation (42a). Note that, when $Ra = 0$ (equilibrium), equation (45) reduces to equation (42a) for the equilibrium structure factor in the Galerkin approximation. The nonequilibrium contribution in equation (45) is proportional to the dimensionless function $\tilde{F}_{\mathrm{NE}}(\tilde{q}, Ra)$, whose expression is quite involved. Of course, it may be cast in the form (44), that separates the contributions from oscillatory and stationary nonequilibrium fluctuations. Namely:

$$\tilde{F}_{\mathrm{NE}}(\tilde{q}, Ra) = \frac{\tilde{F}^{(\mathrm{s})}_{\mathrm{NE}}(\tilde{q}, Ra)}{1 - \dfrac{Ra}{R_{\mathrm{s}}(\tilde{q})}} + \frac{\tilde{F}^{(\mathrm{o})}_{\mathrm{NE}}(\tilde{q}, Ra)}{1 - \dfrac{Ra}{R_{\mathrm{o}}(\tilde{q})}}, \tag{46}$$

where

$$\tilde{F}^{(\mathrm{s})}_{\mathrm{NE}}(\tilde{q}, Ra) = \frac{1 + \psi + \left[Pr\mathcal{R}_T - \dfrac{P_0^2\psi[1 + \psi(1 - \mathcal{R}_D^{-1})]}{LeB(\tilde{q})}\right] Ra}{R_{\mathrm{s}}(\tilde{q})\ [1 + \psi G_0(q)]}, \tag{47a}$$

and

$$\tilde{F}^{(\mathrm{o})}_{\mathrm{NE}}(\tilde{q}, Ra) = \frac{1 + \psi D_4(\tilde{q}) + \mathcal{R}_T PrRa}{R_{\mathrm{o}}(\tilde{q})\ [1 + \psi D_3(q)]} - \frac{\tilde{F}^{(\mathrm{s})}_{\mathrm{NE}}(\tilde{q}, Ra)}{R_{\mathrm{o}}(\tilde{q})}, \tag{47b}$$

with

$$D_4(\tilde{q}) = 1 + \frac{2P_0\sqrt{2}}{\pi P_1}\frac{[Pr\ C_2(\tilde{q}) + Le]}{Pr\ C_2(\tilde{q})}, \tag{48a}$$

$$G_0(\tilde{q},\psi) = C_3(\tilde{q}) + \frac{C_1(\tilde{q})[C_3(\tilde{q}) - D_3(\tilde{q})]}{P_1^2 C_4(\tilde{q}) - C_1(\tilde{q})}. \tag{48b}$$

Similarly to equation (41) for $\mathcal{R}_D$, we have introduced a dimensionless ratio between the strengths of the random stress tensor and of the random heat flow:

$$\mathcal{R}_T = \frac{a^2 c_p}{\alpha^2 g^2 L^4 T}. \tag{49}$$

The functions $D_4(\tilde{q})$ and $G_0(\tilde{q},\psi)$ defined in equation (48) are always positive and have finite limits at $\tilde{q} \to \infty$. When $\tilde{q} \to 0$, $D_4(\tilde{q})$ (as all previous D functions) reaches a finite limit, while $G_0(\tilde{q},\psi)$ diverges proportionally to $\tilde{q}^{-4}$.

Next we proceed to discuss equations (46-47). First of all, we observe that, when condition (35) holds, we encounter a divergence in the first term of the RHS of equation (46). Consequently, our expression for $S^{\rm NE}_{\theta\theta}(\tilde{q})$ is only valid for Ra values up to the $Ra_{\rm c,s}$ obtained from equation (35). In addition, a second divergence is found in the second term of the RHS of equation (46), which corresponds to the Hopf instability (36). As is well known [9], when $\psi > 0$, the Hopf instability is secondary with respect to the (primary) stationary instability. Thus, the divergence associated with the Hopf mode occurs at Ra values larger than the $Ra_{\rm c,s}$ obtained from (35), so that the Ra interval of validity of equation (46) is not changed (for $\psi > 0$), in spite of the presence of a second instability mechanism.

As was elucidated earlier, all the C functions, as well as the D functions, have finite limiting values for $q \to \infty$. Consequently, the behavior of the structure factor in this limit will be dominated by the inverse of the $R_{\rm s}(q)$ and $R_{\rm s}(q)$ functions, appearing in the denominators of equations (47). Hence, taking the difference between equations (45) and (42a), we find that the enhancement of nonequilibrium fluctuations in the large q limit is proportional to $\tilde{q}^{-4}$, namely:

$$S^{\rm NE}_{\theta\theta}(\tilde{q}) \xrightarrow{q\to\infty} S^{(\rm NE,\infty)}_{\theta\theta}\ \frac{1}{\tilde{q}^4} + \mathcal{O}(\tilde{q}^{-6}), \tag{50}$$

with

$$\frac{S^{(\rm NE,\infty)}_{\theta\theta}}{S^{\rm E}_{\theta\theta}} = \frac{P_1^2\ Pr}{Pr+1} \times \left[1 + \frac{\psi\left(Le + 1 - \frac{2\sqrt{2}P_0}{\pi P_1}\right)}{Le+1} + Pr\mathcal{R}_T Ra\right], \tag{51}$$

where $S^{\rm E}_{\theta\theta}$ is the same equilibrium contribution given by equation (42a). In equations (50) and (51) we have added the contributions from the stationary and from the oscillatory fluctuations, in order to obtain a more compact expression. At large q, boundary effects are negligible, so that equation (50) may be compared with the result obtained by performing a full spatial Fourier transform, similar to the procedure explained in Section 5 for the equilibrium fluctuations. A calculation of such a "bulk" structure factor, using a definition like equation (50), would result in [12]

$$\frac{S^{(\rm NE,\infty)}_{\theta\theta}}{S^{\rm E}_{\theta\theta}} = \frac{Pr}{Pr+1}\left[1 + \frac{\psi Le}{Le+1} + Pr\mathcal{R}_T Ra\right], \tag{52}$$

where $S^{\rm E}_{\theta\theta}$ now represents the exact "bulk" contribution, as given by equation (39). Equation (52) is the expected exact result, to be compared with equation (51), which is what was obtained from our Galerkin approximation. We notice two differences: first, the presence of an overall prefactor $P_1^2 \approx 0.973$ which is a 3% lower than the expected value; second, a term $1 - 2\sqrt{2}P_0/\pi P_1 \approx 0.242$, which is close to the expected zero value. The fact that these two differences are small supports again the validity of our Galerkin approximation.

The other interesting limit is $q \to 0$. Similarly to the large-q limit discussed in the previous paragraph, from the first-order Galerkin approximation with rigid and impermeable boundaries, equation (47), we obtain for the nonequilibrium enhancement for small q:

$$\frac{S^{\rm NE}_{\theta\theta}(\tilde{q})}{S^{\rm E}_{\theta\theta}} \xrightarrow{\tilde{q}\to 0} \frac{P_1^2 Pr}{16\Lambda^4}\frac{1 + \left(1 - \frac{2\sqrt{2}P_0}{\pi P_1}\right)\psi + \mathcal{R}_T PrRa}{Pr + \frac{P_0\pi^2(P_0\Lambda^2 - 8)}{16\Lambda^2}}\ \tilde{q}^2 + \mathcal{O}(\tilde{q}^4). \tag{53}$$

In this case the "bulk" structure factor, *i.e.*, without considering boundary conditions, predicts a finite nonzero value of the enhancement at $q \to 0$. Thus, the boundary conditions (vanishing temperature fluctuations at the walls) causes the enhancement of the nonequilibrium temperature fluctuations to vanish at small q.

Another limiting case that is worth studying is $\psi = 0$, in which case our problem reduces to the Rayleigh-Bénard problem for a one-component fluid, which has been considered in a previous publication [6], where a different set of Galerkin test functions was employed. Simply setting $\psi = 0$ in equations (45) and (47), we obtain

$$S_{\theta\theta}(\tilde{q}) = S^{\rm E}_{\theta\theta}\left[1 + \frac{PrRa}{Pr + \frac{C_1(\tilde{q})}{C_2(\tilde{q})}\frac{1 + Pr\mathcal{R}_T Ra}{\frac{C_1(\tilde{q})B(\tilde{q})}{P_1^2} - Ra}}\right], \tag{54}$$

to be compared with equation (25) in reference [6]. From such a comparison, we first find that the result obtained for the equilibrium structure factor (substituting $Ra = 0$ in Eq. (54)) is a 19% lower than the exact "bulk" result, equation (39), while with the Galerkin test functions used in previous publications [6,2], the approximation for the equilibrium structure factor was 17% lower. Secondly, the critical Rayleigh number obtained from (54) is $R_{\rm c} = 1728$ [30], which agrees better with the true

$R_c = 1708$ than the value $R_c = 1750$ obtained from the Galerkin test functions employed in reference [6]. On the other hand, the behavior for large q obtained from equation (54) is a 21% lower than the true asymptotic value, to be compared with a 20% difference obtained from the Galekin test functions used in reference [6]. It is thus difficult to say which of the two sets of Galerkin test functions are best for the representation of the nonequilibrium structure factor. We conclude that, since equation (54) gives a best approximation for Ra_c, it will probably represent best the true nonequilibrium structure factor for q values close to q_c.

From the asymptotic behaviors, equations (50) and (53), we note that the nonequilibrium enhancement exhibits a crossover from a $\tilde{q}^{-4}$ behavior at large $\tilde{q}$ to a $\tilde{q}^2$ behavior at small $\tilde{q}$. This implies that, at least, there will be a local maximum for some nonzero wave number $\tilde{q}_m$. However, the most interesting thing is that, depending on ψ and Ra, the amplitude of nonequilibrium temperature fluctuations may display two maxima, implying a bimodal distribution of the nonequilibrium fluctuations as a function of $\tilde{q}$. The two maxima correspond to the two competing instability mechanisms (Rayleigh and Hopf). This is clearly shown in Figure 1, where we have plotted as a function of $\tilde{q}$ and for two Ra numbers, the amplitude of nonequilibrium temperature fluctuations, normalized to the coefficient multiplying $\tilde{q}^{-4}$ in the asymptotic expansion for large $\tilde{q}$. The data in Figure 1 correspond to $Le = 0.015$, $Pr = 4.16$ and $\psi = 0.025$, which are quite reasonable numbers for ordinary liquid mixtures. Additionally, the data in Figure 1 are for $\mathcal{R}_D = 10^{-3}$ and $\mathcal{R}_T = 5$; these values are also quite reasonable for liquid mixtures, although the final shape of the curve does not depend very much on the values chosen for these two parameters. The solid curve in Figure 1 corresponds to $Ra = 419$, which is approximatively $Ra \approx 0.99 Ra_{c,s}$ for the quoted values of Pr, Le and ψ, while the dotted curve corresponds to $Ra = 0.5 Ra_{c,s}$. In Figure 1 the appearance of a bimodal structure factor as the instability is approached is evident. For the larger Ra, the right broader maximum (at higher values of $\tilde{q}$) is caused by Hopf fluctuations, while the left sharper maximum is caused by Rayleigh fluctuations. For the data displayed in Figure 1, as $Ra \to Ra_{c,s}$, a divergence will appear at the position $\tilde{q}_{c,s}$ of the left maximum. For the lower Ra value, the broad maximum corresponding to Hopf fluctuations masks the second maximum corresponding to Rayleigh fluctuations.

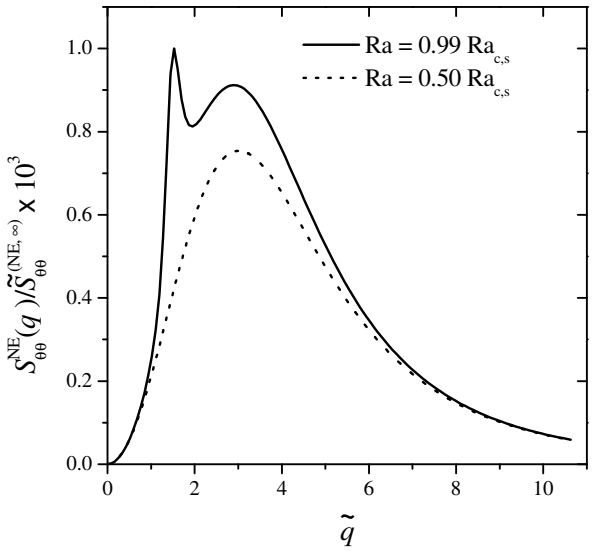

Fig. 1. Appearance of a bimodal distribution for the amplitude of nonequilibrium temperature fluctuations as the stationary instability is approached. The broad peak corresponds to the Hopf fluctuations, while the sharper peak to the left for larger Ra corresponds to the Rayleigh fluctuations. Parameter values are quoted in the text.

6.2 Concentration fluctuations

Concentration fluctuations are not present in the case of a pure fluid. In the case of a binary mixture, they are usually easier to observe than temperature fluctuations [32, 33]. Consequently, it is important to derive an expression for the concentration fluctuations. Here, we may calculate the amplitude of the nonequilibrium concentration fluctuations from the temperature autocorrelation, the ζ-variable autocorrelation, and the cross-correlation between temperature and ζ fluctuations, remembering that $\Gamma = \beta^{-1}[\zeta - \psi\alpha\theta]$. The result may be cast in a form similar to equations (43) and (44) for the autocorrelation of ζ fluctuations, so as to identify the independent contributions from the Hopf and the Rayleigh mechanisms. This requires a lot of algebra, and the resulting expressions are very long, considerably longer than those for the temperature fluctuations discussed above. For this reason, we prefer to discuss here the concentration fluctuations graphically and numerically to elucidate the physical features of the results obtained for the concentration fluctuations.

The final result of our calculations for the amplitude of the nonequilibrium concentration fluctuations is shown in Figure 2, where we have plotted the amplitude of the nonequilibrium concentration fluctuations as a function of $\tilde{q}$ for three values of Ra and with all other coefficients constant. Again, the data in Figure 2 have been normalized in terms of the coefficient multiplying $\tilde{q}^{-4}$ in the asymptotic expansion for large $\tilde{q}$, $S_{\Gamma\Gamma}^{(\mathrm{NE},\infty)}$, defined in a way similar to $S_{\theta\theta}^{(\mathrm{NE},\infty)}$ in equation (50) for the temperature fluctuations. Then, the three sets of data displayed go asymptotically as $\tilde{q}^{-4}$ for large $\tilde{q}$. The solid curve corresponds to the same set of parameters for which the temperature fluctuations were displayed in Figure 1 as a solid curve. The dotted curve also corresponds to the same set of parameters, except the Rayleigh number, for which a large and negative value was chosen, $Ra = -1500$, corresponding to the the overstable situation investigated in some experiments [34]. The dashed curve corresponds to a Ra number close to zero, which represents thermal nonequilibrium in microgravity. From a close examination of the data displayed in the figure, as well as from further numerical and analytical investigations, we arrive at the following conclusions:

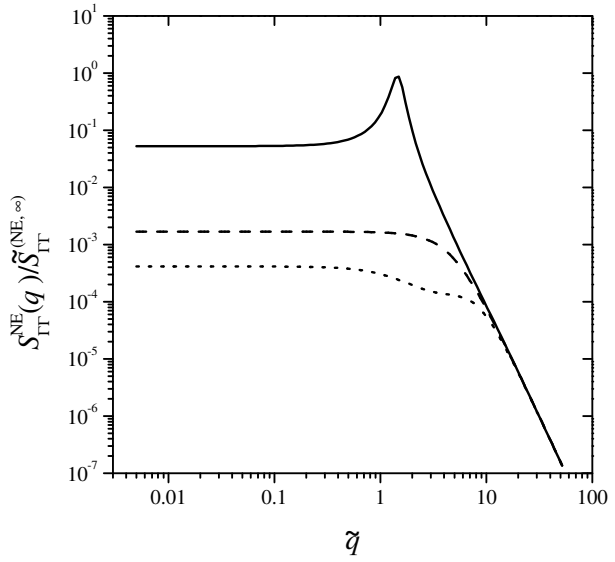

Fig. 2. Normalized amplitude of nonequilibrium concentration fluctuations as a function of $\tilde{q}$, for three values of Ra. The solid curve is for $Ra = 419$, which is close to the $Ra_{c,s}$. The dashed curve is for $Ra \approx 0$, which corresponds to thermal nonequilibrium in microgravity. The dotted curve is for large and negative Rayleigh number $Ra = -1500$, as have been used in some experiments [34].

1. The presence of two maxima which was so evident in Figure 1 for the nonequilibrium temperature fluctuations is masked in the concentration fluctuations. Notice that the solid curve in Figure 2 is for the same Ra number as for the solid curve of Figure 1. We believe this feature is mainly a consequence of the fact that, for usual binary fluids, the Le number is small, so that the contribution of Hopf fluctuations to concentration fluctuations is negligible. This point will be discussed in more detail in Section 7.

2. Most importantly, the amplitude of nonequilibrium concentration fluctuations does not go to zero at $\tilde{q} \to 0$, contrary to the case of the nonequilibrium temperature fluctuations. For concentration fluctuations the nonequilibrium contribution reaches a constant limit at $\tilde{q} \to 0$, for any Ra number. This behavior is due to the different kind of boundary conditions: null derivative instead of null function itself. This explanation is confirmed by a previous investigation [8], where for mathematical simplicity the unrealistic case of two free and permeable walls (implying no concentration fluctuations at the boundaries), was considered. In that case [8], the equivalent $S^{\rm NE}_{\Gamma\Gamma}(\tilde{q})$ vanished at $\tilde{q} \to 0$.

3. As a consequence of #2, below a certain Ra number, the maximum enhancement is reached at $\tilde{q} = 0$. This seems evident in the plots for negative or small Ra in Figure 2. Note that this is never true for the temperature fluctuations.

The constant limit at $q \to 0$ of the nonequilibrium enhancement of concentration fluctuations may be analytically evaluated within the Galerkin approximation employed in this paper. We obtain

$$S^{\rm NE}_{\Gamma\Gamma}(\tilde{q}, Ra) \xrightarrow{\tilde{q}\to 0} \frac{k_{\rm B}T\xi_3}{\rho\beta^2 L^4} Ra \frac{P_0^2(\psi + Pr\mathcal{R}_T\mathcal{R}_D Ra)}{Le\Lambda^4 - \psi P_0^2 Ra}. \quad (55)$$

In Figure 2, for the case of large and negative Ra number, a small dip in the amplitude of the nonequilibrium fluctuations appears for $\tilde{q}$ values close to the ones where, for positive Ra, there appears the maximum associated with the stationary convective instability. It is difficult to assess whether such a small dip is real or is an artifact of the Galerkin approximation. Further work will be necessary to clarify this point.

7 Small-Lewis-number approximation for $\psi > 0$

In the previous section, we have shown how one can derive complete expressions for the nonequilibrium structure factor for arbitrary values of Le, Pr and Ra. However, even with our simple Galerkin approach, such expressions are rather long and complicated; thus a practical and simple approximation would be useful. To obtain such a simple approximation, as usual [35], we take advantage of the separation in order of magnitude of the various diffusivities, since for commonly used liquid mixtures $\nu \gg a \gg D$. Mathematically, we consider $Le = \mathcal{O}(\epsilon)$ and $Pr = \mathcal{O}(\epsilon^{-1})$ in some small parameter ϵ. Additionally it should be recalled that the Rayleigh number is proportional to ν^{-1}, so that $Ra = \mathcal{O}(\epsilon)$. This kind of approximation means considering our system subjected to a given value of ∇T_0 (always below the instability), and taking the leading term in the small parameter ϵ. Following previous authors [36], we refer to this approximation scheme as a small-Lewis-number approximation. For instance, if we replace in equations (35) and (36), Pr by Pr/ϵ, Le by $Le\ \epsilon$, and Ra by $Ra\ \epsilon$, expanding in ϵ, we readily obtain

$$1 - \frac{Ra}{R_{\rm s}(q)} = 1 - \frac{P_0^2 \psi Ra}{B(\tilde{q})\ Le} + \mathcal{O}(\epsilon), \quad (56a)$$

$$1 - \frac{Ra}{R_{\rm o}(\tilde{q})} = 1 + \mathcal{O}(\epsilon). \quad (56b)$$

Of course, we recognize in the LHS of equations (56) the denominators appearing in the general expression of the amplitude of nonequilibrium fluctuations, equation (44). We conclude from equation (56) that, in zeroth-order approximation, the divergence associated with the Hopf bifurcation disappears, while the divergence associated with Rayleigh bifurcation remains. Thus, our small-Lewis-number approximation neglects the oscillatory instability, since there is no divergence when $Ra_{\rm c,o}$ is approached. Next, we perform the same kind of expansion for the amplitudes of the Rayleigh and Hopf fluctuations in the ζ-variable. The leading terms are

$$S^{(\rm s)}_{\zeta\zeta}(\tilde{q}, Ra) = \mathcal{O}(\epsilon^{-1}), \qquad S^{(\rm o)}_{\zeta\zeta}(\tilde{q}, Ra) = \mathcal{O}(1). \quad (57)$$

In this expansion the dimensionless ratios, $\mathcal{R}_D$ and $\mathcal{R}_T$, are taken as $\mathcal{O}(1)$. From equations (56) and (57), we conclude that the amplitude of the Hopf nonequilibrium ζ fluctuations is negligible compared to the amplitude of the Rayleigh nonequilibrium ζ fluctuations. Performing similar expansions for the amplitudes of the temperature fluctuations, and for the amplitudes of the T-ζ cross fluctuations, we find that they contribute, at most, as $\mathcal{O}(1)$. Therefore the dominant contribution to the nonequilibrium concentration fluctuations is given by $S^{(\mathrm{s})}_{\zeta\zeta}(\tilde{q}, Ra)$ in this small-Lewis-number limit. Neglecting any other contribution, expanding $S^{(\mathrm{s})}_{\zeta\zeta}(\tilde{q}, Ra)$ up to $\mathcal{O}(\epsilon^{-1})$ and the corresponding denominator (56a) up to $\mathcal{O}(\epsilon)$, and, finally, substituting $\epsilon = 1$, we obtain a rather simple expression for the amplitude of the nonequilibrium concentration fluctuations:

$$S^{\mathrm{NE}}_{\Gamma\Gamma}(\tilde{q}, Ra) = \frac{k_{\mathrm{B}}T\xi_3}{\rho\beta^2 L^4} \frac{\dfrac{P_0^2 Ra}{LeB(\tilde{q})}\left[\psi + Pr\mathcal{R}_T\mathcal{R}_D Ra\right]}{1 - \dfrac{P_1^2 Ra}{B(\tilde{q})C_1(\tilde{q})}\left[1 + \psi C_3(\tilde{q})\right]}, \quad (58)$$

where $C_3(\tilde{q})$ was defined in equation (33). Approximation (58) exhibits the correct asymptotic behaviors for both large and small $\tilde{q}$. Thus, it reaches a finite nonzero limit at $\tilde{q} \to 0$ and it is proportional to $\tilde{q}^{-4}$ for large $\tilde{q}$. The proportionality coefficient of the large $\tilde{q}$ limit, similar to the one defined in equation (50) for the temperature fluctuations, is easily evaluated as

$$S^{(\mathrm{NE},\infty)}_{\Gamma\Gamma} = \frac{k_{\mathrm{B}}T\xi_3}{\rho\beta^2 L^4} \frac{P_0^2 Ra}{Le}\left[\psi + Pr\mathcal{R}_T\mathcal{R}_D Ra\right]. \quad (59)$$

Some further observations about equation (58) are worth mentioning: First of all, we would like to stress that the ϵ-expansion leading to equation (58) is completely systematic, except for the fact that we expanded the Rayleigh instability condition in the denominator up to $\mathcal{O}(\epsilon)$, instead of retaining only the leading $\mathcal{O}(1)$ term. We have proceeded in this way because it greatly improves the approximation, particularly for Ra values close to the instability. A completely systematic small-Lewis-number approximation would have given the $\mathcal{O}(1)$ term of the RHS of equation (56a) as the denominator in equation (58). A consequence will be that the maximum (as a function of $\tilde{q}$) of the nonequilibrium structure factor will always be at $\tilde{q} = 0$. As discussed elsewhere [14], this is actually the case when a strict zeroth-order small-Lewis-number approximation is applied to the starting Boussinesq equations. A second consequence will be that the critical Rayleigh number, thus, the Ra value at which nonequilibrium fluctuations diverge, will be no longer given by equation (35). However, one should notice that the structure factor, as given by (58), diverges (for $\psi > 0$) for the same condition (35) obtained for the linear Rayleigh instability within our Galerkin approximation [9], which usually happens at a $q_{\mathrm{c,s}} \neq 0$[2]. This is the main reason why we prefer to expand the denominator up to $\mathcal{O}(\epsilon)$. Also it demonstrates the advantage of having obtained equation (58) from the full set of binary Boussinesq equations (4), instead of having adopted the $Le \to 0$ approximation in the starting equations.

Secondly, it would evidently be highly desirable to have explicit analytical expressions for the value of the wave number of fluctuations maximally enhanced as a function of the Rayleigh and Lewis numbers, and of the separation ratio ψ. However, it turns out that such expressions are quite involved, and a numerical investigation is more useful. This is the same situation encountered by Lhost *et al.* [9] when studying the critical wave number and Rayleigh number, as discussed in Section 4. Though such a numerical investigation may be easily performed from equation (58), we do not pursue this here.

Thirdly, we note that by taking the "bulk" limit (*i.e.*, $P_1 = P_2 = C_1(\tilde{q}) = C_3(\tilde{q}) = 1$, and $B(\tilde{q}) = q^4L^4$) of the strictly systematic version of equation (58), we reproduce exactly a previous result [12] obtained without taking into account boundary conditions, and starting from the linearized binary Boussinesq equations within a small-Lewis-number approximation. This feature of equation (58) is especially important, because the "bulk" limit has been experimentally verified for negative Ra and relatively large q values [12].

Finally, it is important to recall that, in deducing equation (58), we have completely neglected the oscillatory instability. Consequently, equation (58) will be only valid for $\psi > 0$. In the case $\psi < 0$, it happens that, though the amplitude of the Hopf fluctuations is indeed $\mathcal{O}(1)$ in our small-Le expansion, the corresponding denominator is almost zero in the neighborhood of some $\tilde{q}_{\mathrm{c,s}}$, so that the actual contribution of the Hopf fluctuations may be very large. The approximation (58) will be particularly worse for $\psi < 0$ and for $\tilde{q}$ values close to the $\tilde{q}_{\mathrm{c,o}}$ of the Hopf instability. We should also emphasize that neglecting Hopf fluctuations, as was done in equation (58), is only justified for the nonequilibrium concentration fluctuations. For the temperature fluctuations it turns out that the amplitude of the Rayleigh and the Hopf components are of the same order in ϵ. Therefore, both have to be taken into account simultaneously, and this is the reason why the amplitude of the concentration fluctuations shown in Figure 2 for $Ra = 419$ does not exhibit the bimodal distribution found in Figure 1 for the temperature fluctuations at the same Ra.

To illustrate the appropriateness of the approximation (58), we show in Figure 3 a plot of equation (58) for the same parameter values plotted in Figures 1 and 2, that is, $Le\ \epsilon = 0.015$, $Pr/\epsilon = 4.15$, and for two of the values of the Rayleigh number considered in Figure 2: $Ra\ \epsilon = 419$, which is close to the Rayleigh instability, and for $Ra\ \epsilon = -1.5 \times 10^3$, which is a Rayleigh number of the order employed in some experiments [33]. As in previous plots, we have normalized the nonequilibrium structure factors by dividing with the corresponding proportionality constant of the large $\tilde{q}$ asymptotic expansion, $S^{(\mathrm{NE},\infty)}_{\Gamma\Gamma}$. Consequently, all plots in the figure share the

[2] The comments about the value of $\tilde{q}_{\mathrm{c,s}}$ after equation (35) apply here.

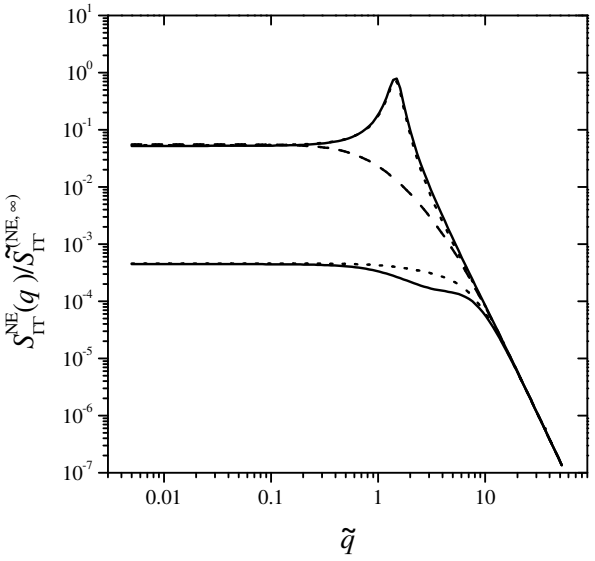

Fig. 3. Various small-Lewis-number approximations to the nonequilibrium amplitude of concentration fluctuations. Solid curves represent full Galerkin results, while dashed or dotted curves represent various small-Le-number approximations (see text).

same asymptotic limit for large $\tilde{q}$. The solid curves in Figure 3 correspond to the full Galerkin expression for the amplitude of the nonequilibrium concentration fluctuations; they are actually the same curves plotted in Figure 2. The dotted curves correspond to the small-Le approximation: equation (58) divided by equation (59). It is evident that the small-Lewis-number approximation represents the full structure factor quite well; actually for Ra close to $Ra_{c,s}$ it is almost undistinguishable from the one obtained in the full Galerkin approximation. Additionally, we have also displayed (dashed curve) the curve that would be obtained with the systematic small-Le approximation (*i.e.*, retaining only the term $\mathcal{O}(1)$ in the denominator of equation (58)). It is evident that, while for Ra close to Ra_c, the approximation (58) clearly improves the strict $Le \to 0$ approximation, for negative values of Ra the difference is completely negligible. Actually, for $Ra = -1500$ the plot of the strict $Le \to 0$ approximation was removed from Figure 3, because it was completely indistinguishable from equation (58) divided by equation (59).

8 Concluding remarks

In this paper, we have employed a simple Galerkin-approximation scheme to calculate the nonequilibrium contribution to the various thermodynamic fluctuations from the linearized binary Boussinesq equations using realistic boundary conditions. The same set of Galerkin test functions has been previously employed by Lhost *et al.* [9] to successfully study the linear instability problem. Since the conclusions of our work may be hidden by the long and cumbersome algebra, we summarize here our main findings.

First of all, the nonequilibrium fluctuations in any thermodynamic variable for the binary Boussinesq problem may be classified as arising from one of the two instability mechanisms present. So it is possible to distinguish between nonequilibrium fluctuations associated with the Rayleigh stationary instability and nonequilibrium fluctuations associated with the Hopf oscillatory instability, see equation (44).

The amplitude of nonequilibrium temperature fluctuations, as a function of the wave number q of the fluctuations, decays as q^{-4} for large q (in accordance with the well-known behavior of the "bulk" structure factor [10]) and goes to zero as q^2 for extremely small q, as previously found for the case of a pure fluid [6]. Between these two limiting behaviors (and close to the stationary instability for $\psi > 0$) the nonequilibrium enhancement of temperature fluctuations may present two maxima, reflecting the presence of two competing instability mechanisms.

Due to the different kinds of boundary condition (null derivative *versus* null function), the nonequilibrium enhancement of concentration fluctuations does not go to zero at $q \to 0$, but it reaches a constant nonzero limit, given by equation (55) in our Galerkin approximation. We conclude that the physical nature of boundary conditions determines the behavior at $q \to 0$ of the corresponding nonequilibrium fluctuations and, in principle, may be experimentally investigated. A consequence is that, for concentration fluctuations at $\psi > 0$, the maximum enhancement is usually at $q = 0$, except for Ra numbers very close to the stationary instability.

Finally, we have derived a simple approximation for the amplitude of the nonequilibrium concentration fluctuations taking advantage of the fact that the Le number is small for common binary mixtures or solutions. We have shown that, for $\psi > 0$, such an approximation is equivalent to neglecting both temperature fluctuations and the fluctuations associated with the Hopf instability. Our simple and systematic $Le \to 0$ approximation compares well with the full nonequilibrium enhancement of the concentration fluctuations for reasonable values of the various thermophysical properties involved.

We acknowledge useful comments received from David S. Cannell, Alberto Vailati and Marzio Giglio.

References

1. M. Wu, G. Ahlers, D.S. Cannell, Phys. Rev. Lett. **75**, 1743 (1995).
2. J. Oh, J.M. Ortiz de Zárate, J.V. Sengers, G. Ahlers, Phys. Rev. E **69**, 021106 (2004).
3. H.N.W. Lekkerkerker, W.G. Laidlaw, J. Phys. (Paris) **38**, 1 (1977).
4. M. Giglio, A. Vendramini, Phys. Rev. Lett. **39**, 1014 (1977).
5. D. Brogioli, A. Vailati, M. Giglio, Phys. Rev. E **61**, R1 (2000).

6. J.M. Ortiz de Zárate, J.V. Sengers, Phys. Rev. E **66**, 036305 (2002).
7. P.N. Segrè, J.V. Sengers, Physica A **198**, 46 (1993).
8. J.V. Sengers, J.M. Ortiz de Zárate, Rev. Mex. Fis. **48** (Supl. 1), 14 (2001).
9. O. Lhost, S.J. Linz, H.W. Müller, J. Phys. II **1**, 279 (1991).
10. B.M. Law, J.C. Nieuwoudt, Phys. Rev. A **40**, 3880 (1989).
11. W. Köhler, S. Wiegand (Editors), *Thermal Nonequilibrium Phenomena in Fluid Mixtures*, Lect. Notes. Phys., Vol. **584** (Springer, Berlin, 2002).
12. J.V. Sengers, J.M. Ortiz de Zárate, in *Thermal Nonequilibrium Phenomena in Fluid Mixtures*, Lect. Notes. Phys., Vol. **584**, edited by W. Köhler, S. Wiegand (Springer, Berlin, 2002) pp. 121-145.
13. C. Normand, Y. Pomeau, M.G. Velarde, Rev. Mod. Phys. **49**, 581 (1977).
14. R.S. Schechter, M.G. Velarde, J.K. Platten, in *Advances in Chemical Physics*, Vol. **26**, edited by I. Prigogine, S.A. Rice (Wiley, New York, 1974) pp. 265-301.
15. M.C. Cross, P.C. Hohenberg, Rev. Mod. Phys. **65**, 851 (1993).
16. S. Chandrasekhar, *Hydrodynamic and Hydromagnetic Stability* (Oxford University Press, Oxford, 1961).
17. R. Schmitz, E.G.D. Cohen, J. Stat. Phys. **39**, 285 (1985).
18. I. Procaccia *et al.*, Phys. Rev. A **19**, 1290 (1979).
19. L.D. Landau, E.M. Lifshitz, *Fluid Mechanics* (Pergamon, London, 1959).
20. I. Pagonabarraga, J.M. Rubí, L. Torner, Physica A **173**, 111 (1991).
21. A.L. Garcia, M. Malek Mansour, G.C. Lie, E. Clementi, J. Stat. Phys. **47**, 209 (1987).
22. J.M. Ortiz de Zárate, J.V. Sengers, J. Stat. Phys. **115**, 1341 (2004).
23. C. Cohen, J.W.H. Sutherland, J.M. Deutch, Phys. Chem. Liquids **2**, 213 (1971).
24. St. Hollinger, M. Lücke, Phys. Rev. E **57**, 4238 (1998).
25. J.M. Ortiz de Zárate, J.V. Sengers, Physica A **300**, 25 (2001).
26. J.M. Ortiz de Zárate, R. Pérez Cordón, J.V. Sengers, Physica A **291**, 113 (2001).
27. J.M. Ortiz de Zárate, L. Muñoz Redondo, Eur. Phys. J. B **21**, 135 (2001).
28. S.P. Trainoff, D.S. Cannell, Phys. Fluids **14**, 1340 (2002).
29. B.J. Berne, R. Pecora, *Dynamic Light Scattering* (Wiley, New York, 1976).
30. J. Niederländer, M. Lücke, M. Kamps, Z. Phys. B **82**, 135 (1991).
31. J.P. Boon, S. Yip, *Molecular Hydrodynamics* (Dover, New York, 1991).
32. W.B. Li *et al.*, Phys. Rev. Lett. **81**, 5580 (1998).
33. W.B. Li *et al.*, J. Chem. Phys. **112**, 9139 (2000).
34. A. Vailati, M. Giglio, Phys. Rev. Lett. **77**, 1484 (1996).
35. P.N. Segrè, R.W. Gammon, J.V. Sengers, Phys. Rev. E **47**, 1026 (1993).
36. M.G. Velarde, R.S. Schechter, Phys. Fluids **15**, 1707 (1972).